

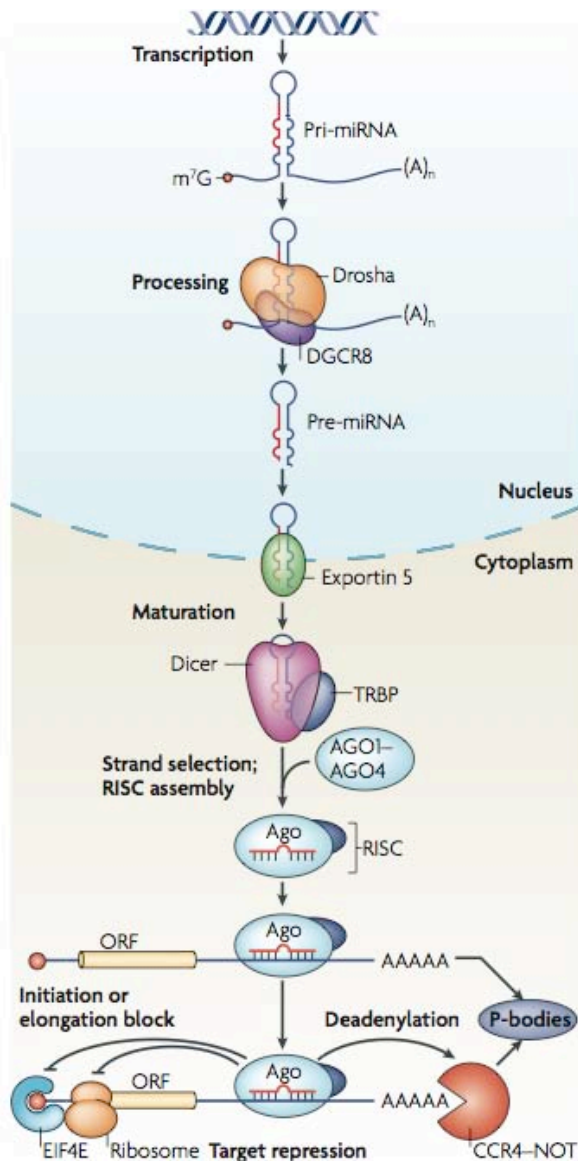
Cours du 21 novembre 2011

MicroRNA control of signal transduction

Inui M, Martello G, Piccolo S

Nat Rev Mol Cell Biol

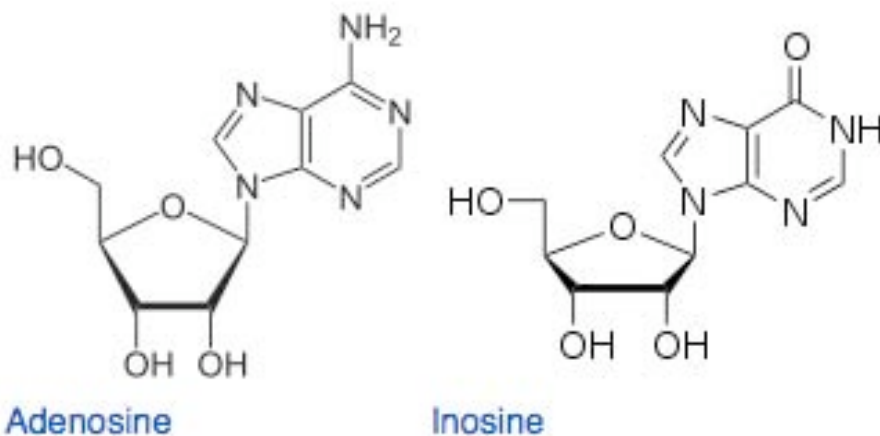
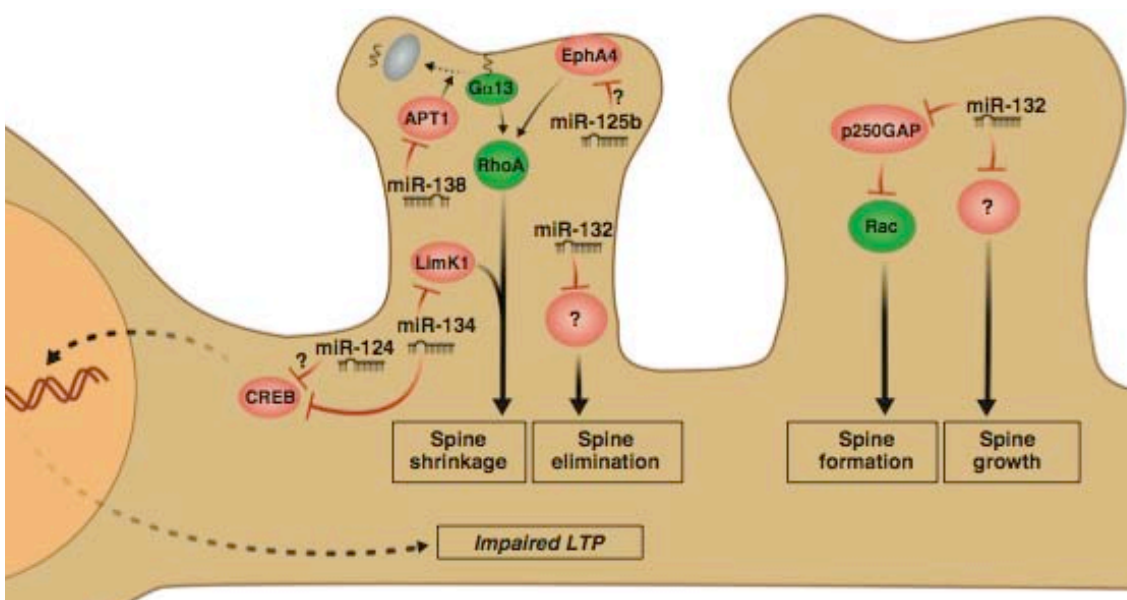
2010 vol. 11 (4) pp. 252-63



microRNAs in neurons: manifold regulatory roles at the synapse

Siegel G, Saba R, Schratt G

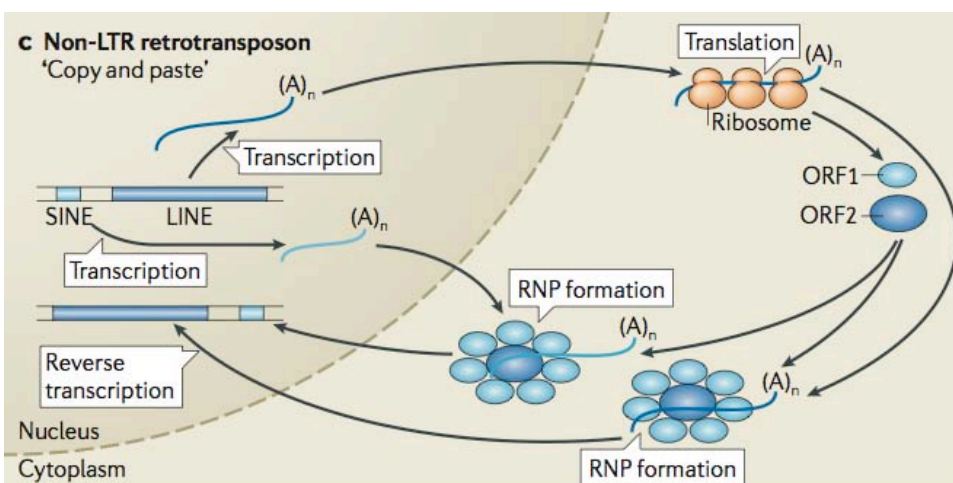
Current Opinion in Genetics &
Development
2011 vol. 21 (4) pp. 491-7



PIWI-interacting small RNAs: the vanguard of genome defence

Nat Rev Mol Cell Biol
2011 vol. 12 (4) pp. 246–58

Somi MC, Sato K, Pezic D, Aravin AA



RNA editing, DNA recoding and the evolution of human cognition

Mattick JS, Mehler MF

Trends in Neurosciences

2008 vol. 31 (5) pp. 227–33

Table 1. Human A-to-I edited DNA repair enzymes: functional roles

| Gene name | Comment | Functional categories |
|--------------------------|---|---------------------------|
| <i>BRCA1</i> | | DSBR (NHEJ, HR); MMR; TCR |
| <i>Claspin</i> | | DSBR (HR) |
| <i>DDB2^a</i> | | NER; GGR; MMR |
| <i>DMC1</i> | Rad51 family | Meiotic HR |
| <i>FANCC^a</i> | | DSBR (HR); TLS |
| <i>FANCD2</i> | | DSBR (HR); TLS |
| <i>MSH2</i> | Mismatch repair enzymes | MMR; DSBR (HR) |
| <i>MSH5</i> | Mismatch repair enzymes | MMR; DSBR (HR) |
| <i>NCAPG^a</i> | | DSBR (NHEJ) |
| <i>NEIL1</i> | | BER; TCR |
| <i>POLM^a</i> | X family DNA polymerases | DSBR (NHEJ); TLS |
| <i>Rad1</i> | | BER; TLS |
| <i>Rad51</i> | | DSBR (HR); TLS |
| <i>RecQL5</i> | | DSBR (HR); NER; TCR |
| <i>Rev3L</i> | Pol- ζ | TLS |
| <i>TOP3A^a</i> | | DSBR (HR); NER; MMR |
| <i>UBE2B</i> | Rad6 homolog; ubiquitin [E2]-conjugating enzyme | TLS |
| <i>USP1^a</i> | | DSBR (HR); TLS |
| <i>XPA^a</i> | | NER; GGR; TCR |
| <i>XPB^a</i> | | NER; GGR; TCR |
| <i>XPV</i> | Pol- η ; Y family DNA polymerases | NER; GGR; TLS |
| <i>XRC6</i> | Ku70 | DSBR (NHEJ) |

Abbreviations: DSBR, double-strand break repair; NHEJ, non-homologous end joining; HR, homologous recombination; NER, nucleotide excision repair; BER, base excision repair; MMR, mismatch repair; GGR, global general repair; TCR, transcription-coupled repair; TLS, trans-lesion synthesis.

^aGene loci specifically verified to have edited transcripts in neural tissues. Supporting information can be found in Refs [38–41].

Box 1. Categories/roles of edited genes involved in nervous system development and function

(a) System-wide adaptations

- i. Neural induction (*SMAD1*; *IFNR1*)
- ii. Anterior (forebrain) neural tube patterning (*FGFR1*; *Formin2*; *HHAT*)

(b) Adaptations of regional neural stem cell functions

- i. Neural stem cell (NSC) self-renewal (*NuMA1*; *CD44*; *SNX1*)
- ii. NSC asymmetric (neurogenic) cell divisions (*Nde1*)
- iii. Modulation of NSC proliferation (*CDC2L5*; *RBBP7*; *PKCD1*; *SYK*)

(c) Adaptations of neuronal precursor (neuroblast) development

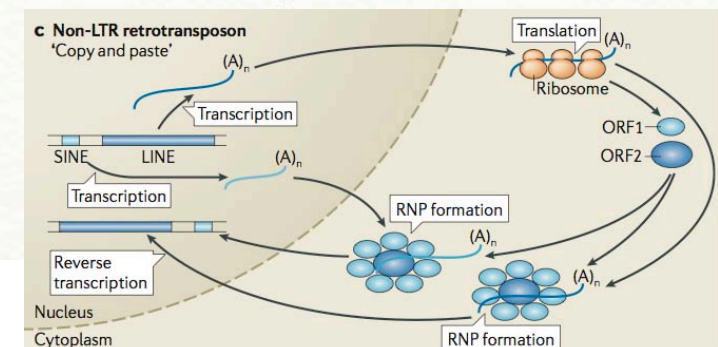
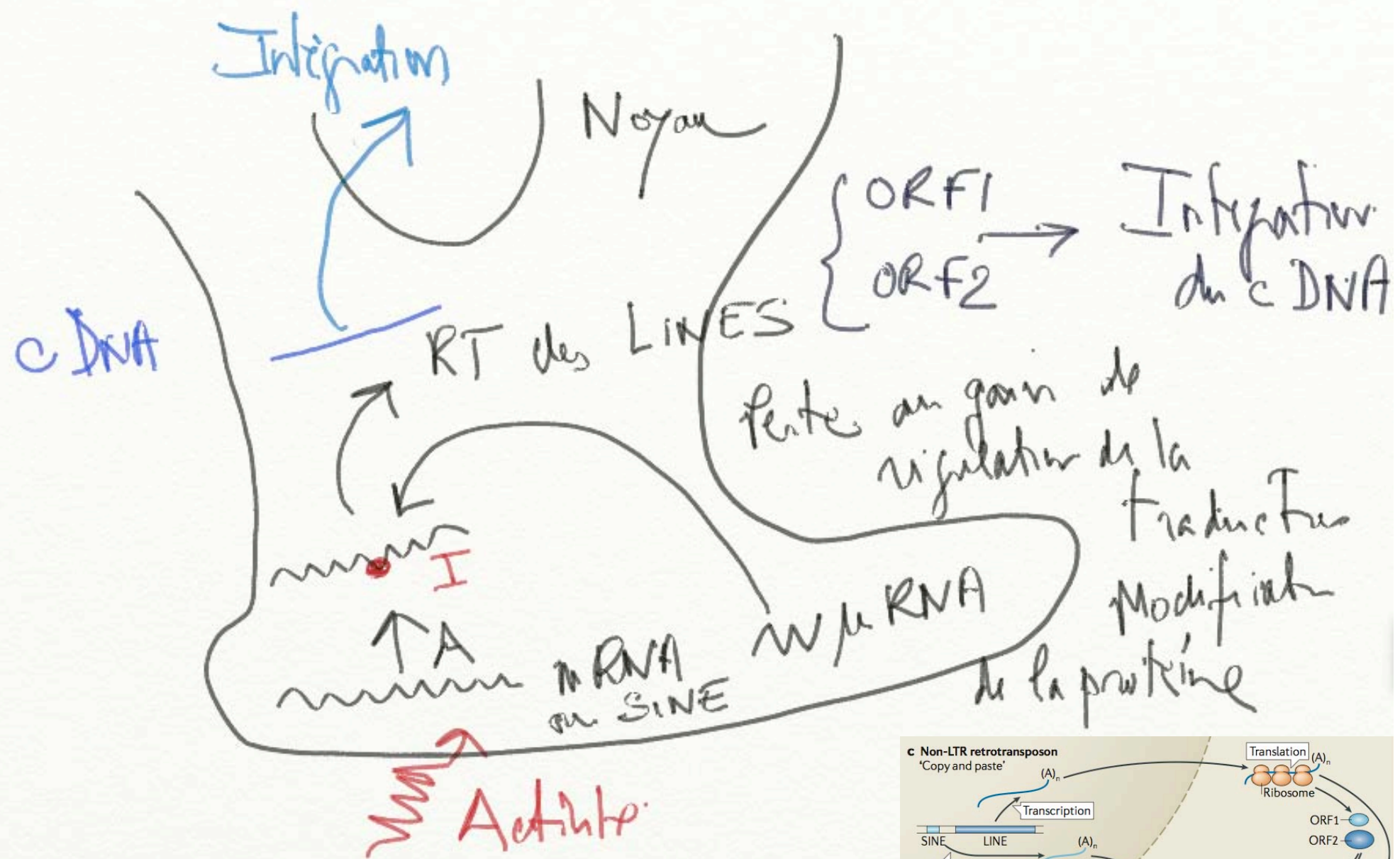
- i. Neuronal precursor (neuroblast; NB) migration (*CXCL1*; *Foxp1*)
- ii. NB cell-cycle kinetics (*Par6*; *CDK10*; *CDKL1*; *MCM3*; *DNM2*; *Cullin1*)
- iii. Modulation of NB cell-cycle exit (*Sox13*)

(d) Adaptations of the process of neuronal maturation

- i. Progressive neuronal differentiation (*TLE2*)
- ii. Neuronal morphogenesis (*PAK4*; *SPARC*)
- iii. Neuronal cell polarity/neurite process outgrowth (*Neuron navigator1*)
- iv. Neuronal axon guidance (*Centaurin- γ 2*)
- v. Neuronal dendritogenesis (β -Catenin)
- vi. Neuronal synaptogenesis (*Protocadherin β*)
- vii. Neuronal subtype specification (*Lhx3*)
- viii. Neuronal network connectivity (*Protocadherin α 1, 2, 4–6, C1, 2*)

(e) Adaptations of mature neuronal functions

- i. Neuronal viability (*Beclin1*; *Casp9, 10*; *TRAP1*; *STAG-1*; Fas inhibitory molecule 1)
- ii. Neuronal excitability (*Annexin A4*; *AMPAR1/GluR1*; *VDCCB4*; *VDKC*)
- iii. Neuronal cell-cell and cell-environment interactions (*Integrin β 4*)
- iv. Cooperative clustering of synaptic neurotransmitter receptors (*VDCC β 2*)
- v. Assembly of multimeric intracellular and cell-cell signaling scaffolds (*Syncoilin*)
- vi. Organization of neuronal somadendritic microdomains (*mGluR1*)
- vii. Neuronal signal transduction (*Src homology domain containing E, SHE*)
- viii. Neuronal plasticity (*CaM Kinase II*; *Synaptotagmin 2*; α -1-Adaptin; *Complexin 1*)
- ix. Neuronal energy metabolism (*CPT1A, C*; *Dynamin1-like*)
- x. Neuronal axodendritic transport (*Kinesin 1B, 2, 3B, 6*; *Dynein 10*)



Human-specific loss of regulatory DNA and the evolution of human-specific traits

McLean CY, Reno PL, Pollen AA, Bassan AI, Capellini TD, Guenther C, Indjeian VB, Lim X, Menke DB, Schaar BT, Wenger AM, Bejerano G, Kingsley DM

Nature
2011 vol. 471 (7337) pp. 216–9

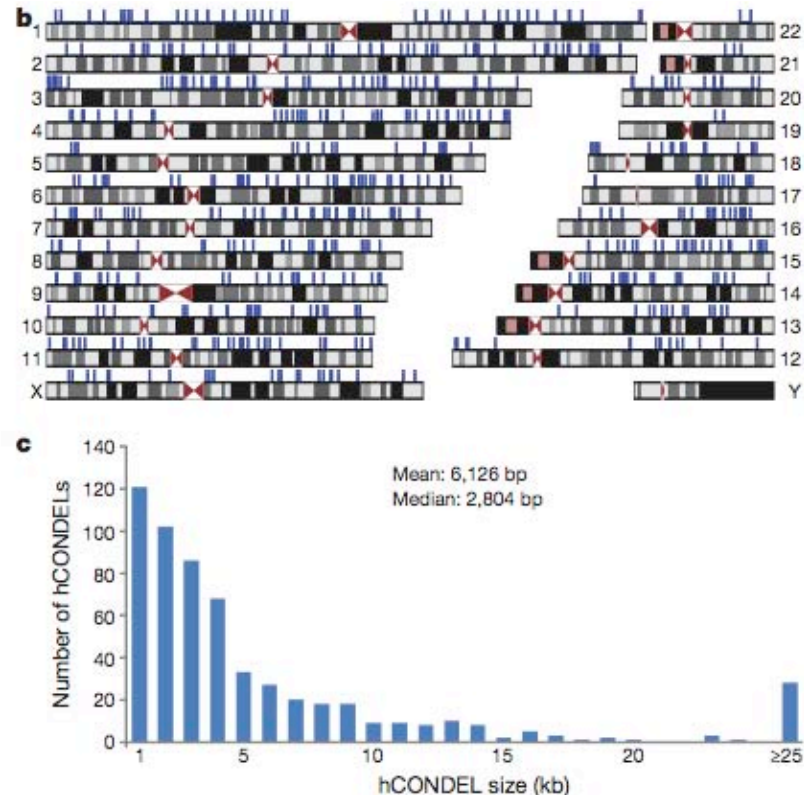
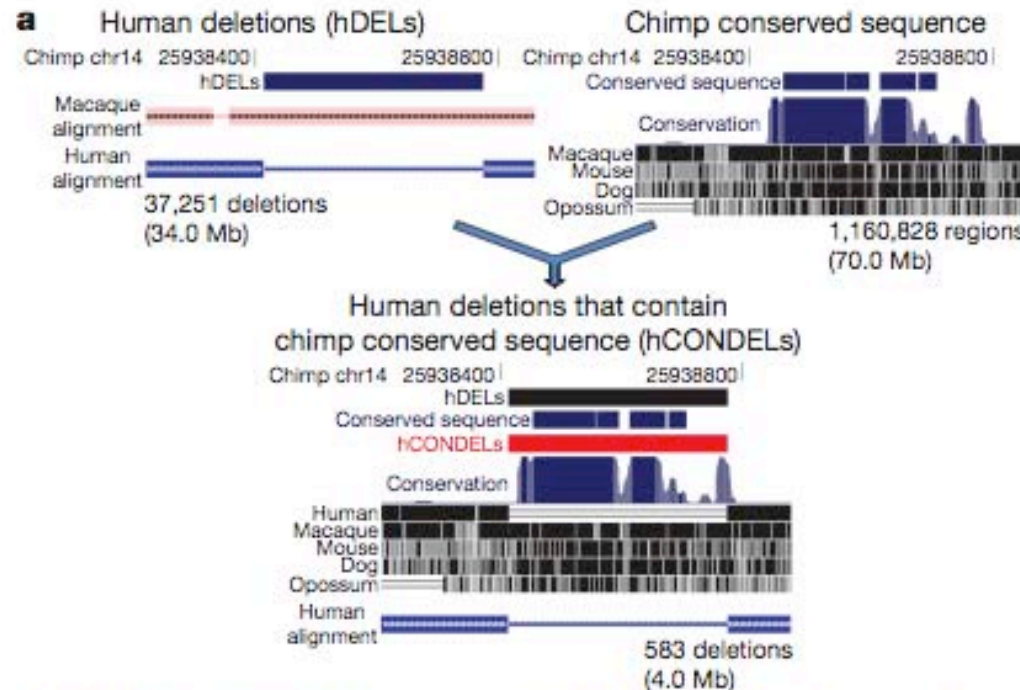
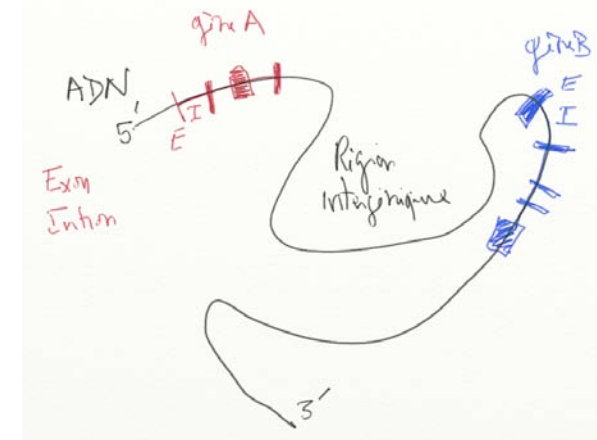


Table 1 | Summary of annotation enrichments of hCONDELs

| Ontology: Term | Expected number of hCONDELs | Observed number of hCONDELs | Fold enrichment | Binomial P-value ¹⁹ |
|--|-----------------------------|-----------------------------|-----------------|--------------------------------|
| GO Molecular Function: Steroid hormone receptor activity | 4.7 | 14 | 2.96 | 3.7×10^{-4} |
| Entrez Gene: Neural genes | 141.3 | 180 | 1.27 | 1.1×10^{-4} |
| MGI Expression in Theiler Stage 21: | | | | |
| Hindbrain | 49.9 | 79 | 1.58 | 3.4×10^{-5} |
| Cerebral cortex | 42.1 | 68 | 1.62 | 7.0×10^{-5} |
| Brain, ventricular layer | 29.9 | 52 | 1.74 | 9.4×10^{-5} |
| Midbrain | 30.5 | 52 | 1.70 | 1.6×10^{-4} |
| InterPro Protein Domains: | | | | |
| Fibronectin, type III | 16.7 | 34 | 2.03 | 1.0×10^{-4} |
| CD80-like, immunoglobulin C2-set | 2.1 | 8 | 3.84 | 1.4×10^{-3} |

Showing only non-redundant terms that are enriched after accounting for both multiple testing and for the tendency of conserved elements to be found near particular classes of genes (Supplementary Information).



Human-specific loss of regulatory DNA and the evolution of human-specific traits

McLean CY, Reno PL, Pollen AA, Bassan AI, Capellini TD, Guenther C, Indjeian VB, Lim X, Menke DB, Schaar BT, Wenger AM, Bejerano G, Kingsley DM

Nature

2011 vol. 471 (7337) pp. 216-9

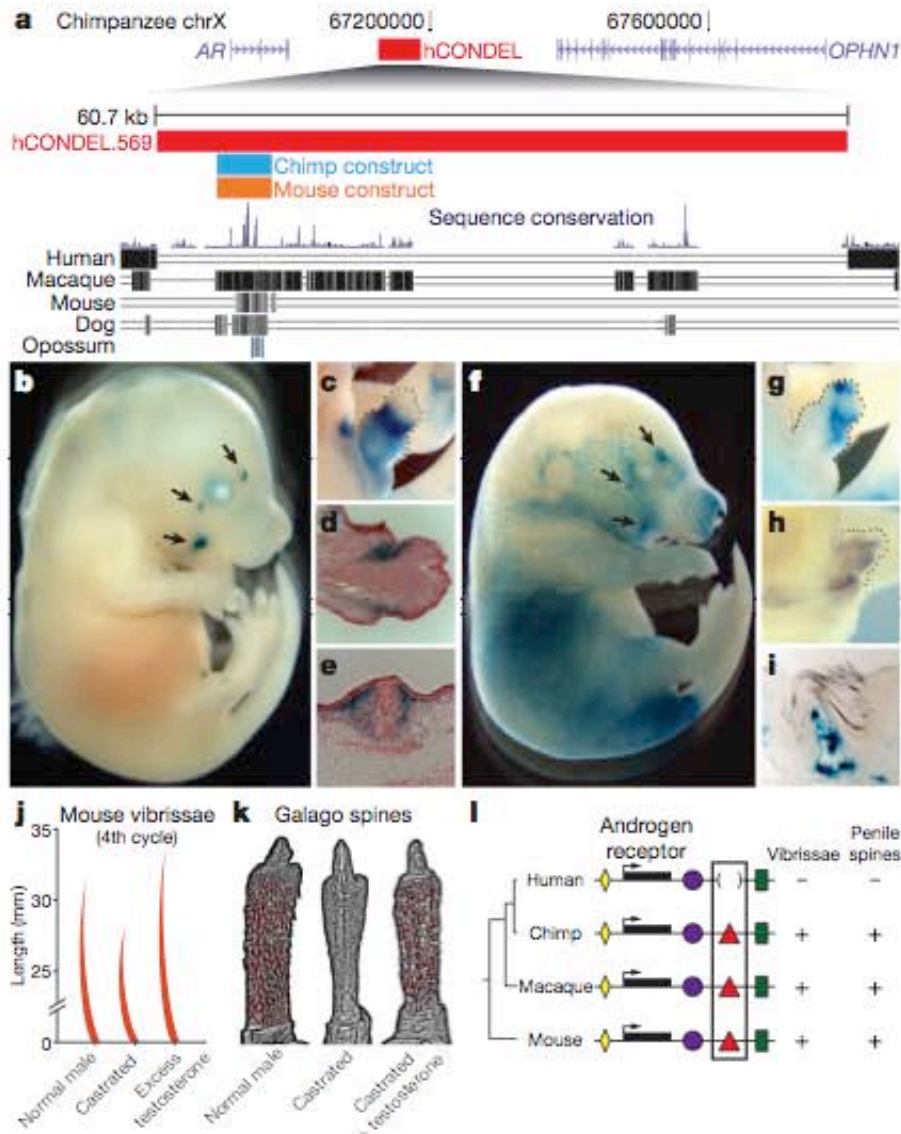
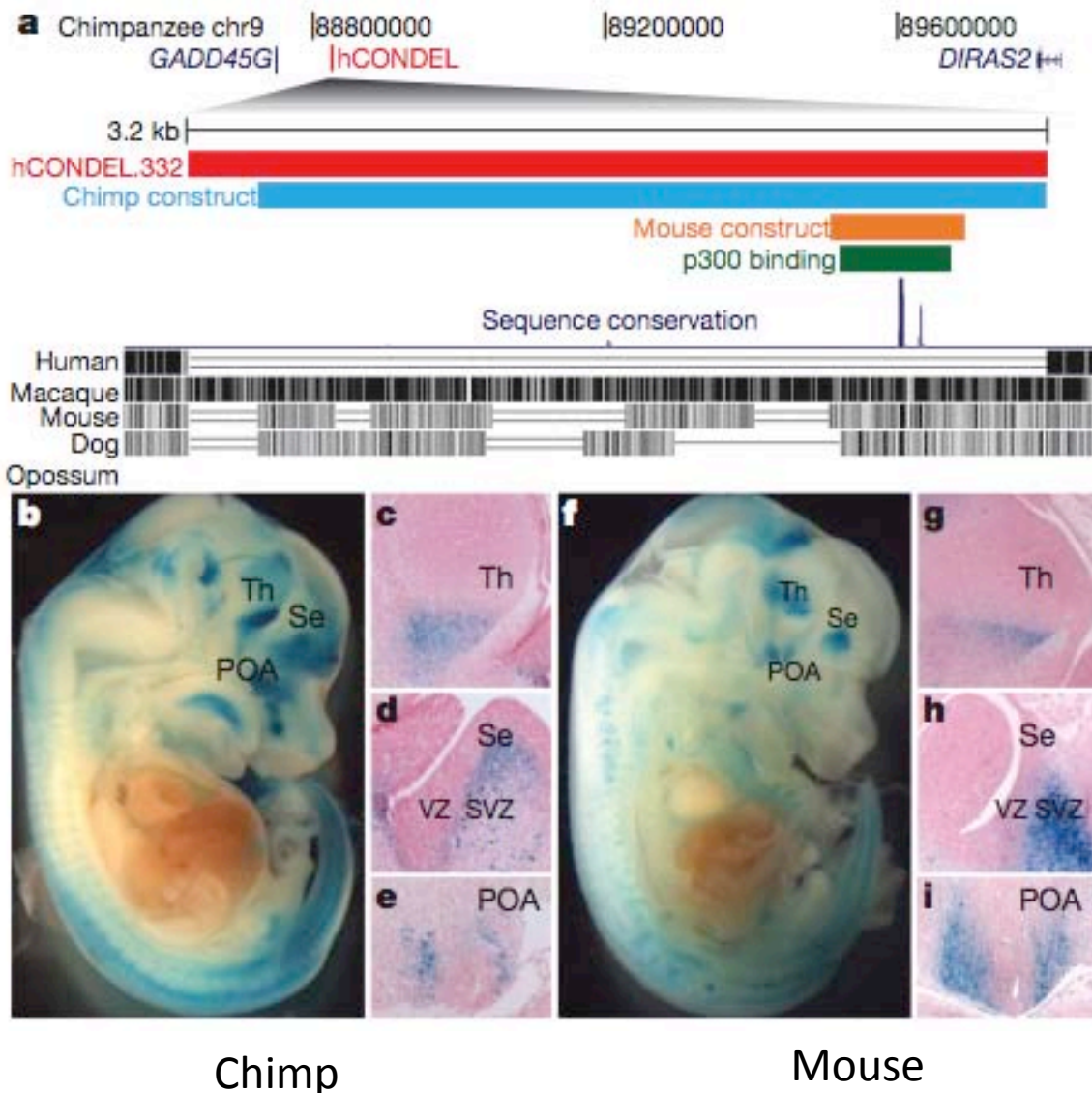


Figure 2 | Transgenic analysis of a chimpanzee and mouse AR enhancer region missing in humans. **a**, Top panel: 1.1 Mb region of the chimpanzee X chromosome. The red bar shows the position of a 60.7-kb human deletion removing a well-conserved chimpanzee enhancer between the AR and OPHN1 genes. Bottom panel: multiple species comparison of the deleted region, showing sequences aligned between chimpanzee and other mammals. Blue and orange bars represent chimpanzee and mouse sequences tested for enhancer activity in transgenic mice. The chimpanzee sequence drives lacZ expression in **b**, facial vibrissae (arrows), and **c**, genital tubercle (dotted line) of E16.5 mouse embryos. Histological sections reveal strongest staining in superficial mesenchyme of **d**, the prospective glans of the genital tubercle, and **e**, dermis surrounding the base of sensory vibrissae. The mouse enhancer also drives consistent expression in **f**, facial vibrissae, **g**, genital tubercle, and hair follicles of E16.5 embryos. **h**, Endogenous AR is expressed in the genital tubercle (dotted line) as demonstrated by *in situ* hybridization. **i**, Histological section of a 60-day-old transgenic mouse penis showing postnatal lacZ expression in dermis of penile spines. Vibrissae and penile spines are androgen-dependent, as shown by **j**, changes in vibrissae length in castrated and testosterone-treated mice and **k**, loss and recovery of penile spines of a castrated and testosterone-treated primate (*Galago crassicaudatus*) (modified from refs 23 and 24). **l**, Model depicting multiple conserved tissue-specific enhancers (coloured shapes) surrounding AR coding sequences (black bars) of different species. Loss of an ancestral vibrissae/penile spine enhancer in humans is correlated with corresponding loss of sensory vibrissae and penile spines.

tion in our species relative to chimpanzees²⁰. This fits with an adaptive suite, including feminization of the male canine dentition, moderate-sized testes with low sperm motility, and concealed ovulation with permanently enlarged mammary glands²⁰, that suggests our ancestors evolved numerous morphological characteristics associated with pair-bonding and increased paternal care²¹.



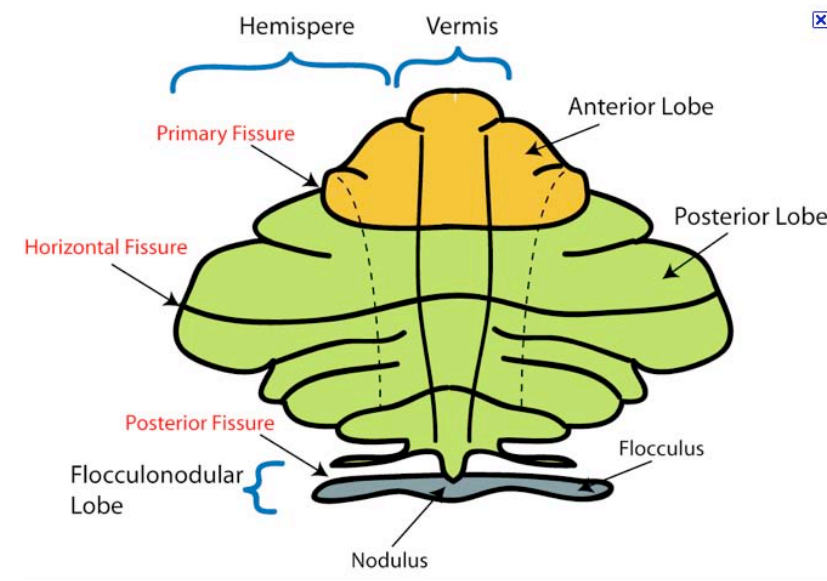
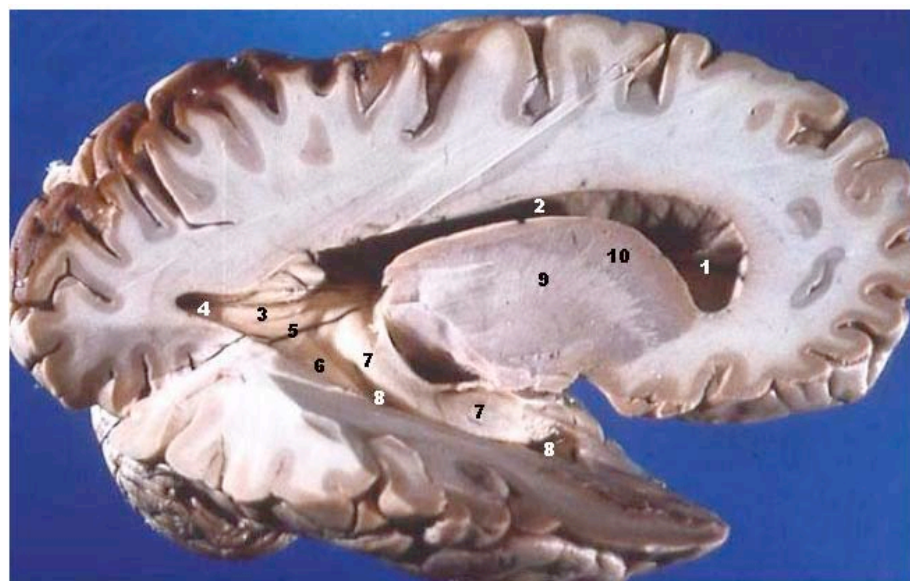
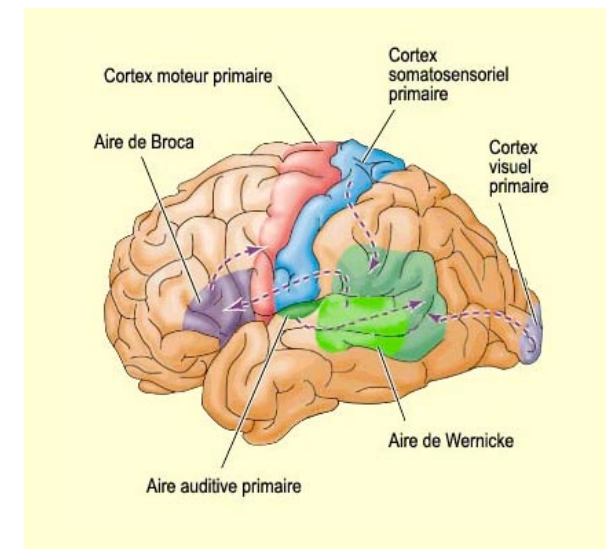
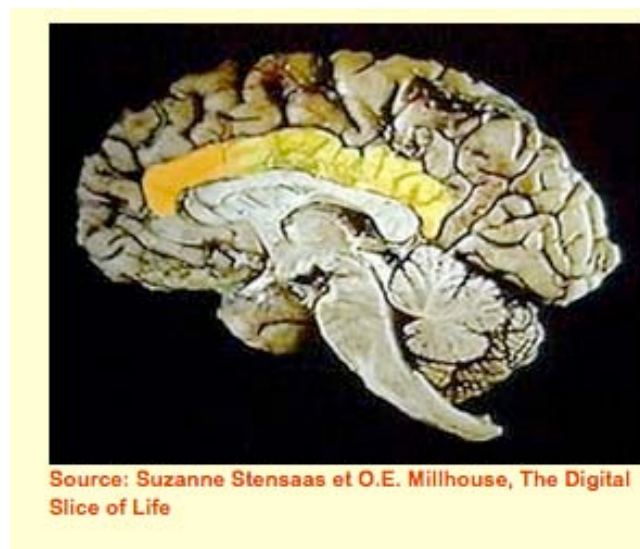
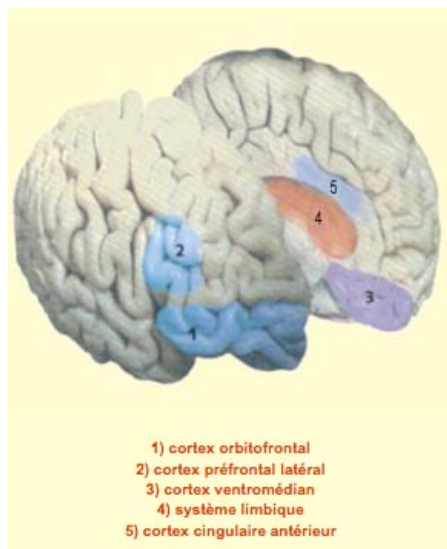
Human-specific loss of regulatory DNA and the evolution of human-specific traits

McLean CY, Reno PL, Pollen AA, Bassan AI, Capellini TD, Guenther C, Indjejian VB, Lim X, Menke DB, Schaar BT, Wenger AM, Bejerano G, Kingsley DM

Nature

2011 vol. 471 (7337) pp. 216-9

Figure 3 | Transgenic analysis of a chimpanzee and mouse forebrain enhancer missing from a tumour suppressor gene in humans. **a**, Top panel: 1.3 Mb region of the chimpanzee chromosome 9. The red bar illustrates a 3,181 bp human-specific deletion removing a conserved chimpanzee enhancer located downstream of *GADD45G*. Bottom panel: multiple species comparison of the deleted region, showing sequences aligned between chimpanzee and other mammals. The green bar represents a mouse forebrain-specific p300 binding site¹⁸, and the blue and orange bars represent chimpanzee and mouse sequences tested for enhancer activity in transgenic mice. The chimpanzee (**b–e**) and mouse sequence (**f–i**) both drive consistent *lacZ* expression in E14.5 mouse embryos in the ventral thalamus (**c, g**), the SVZ of the septum (**d, h**), and the preoptic area (**e, i**). Increased production of neuronal subtypes from these regions may contribute to thalamic and cortical expansion in humans^{27–30}. All sections are sagittal with anterior to right. POA, preoptic area; Se, septum; SVZ, subventricular zone; Th, thalamus; VZ, ventricular zone.



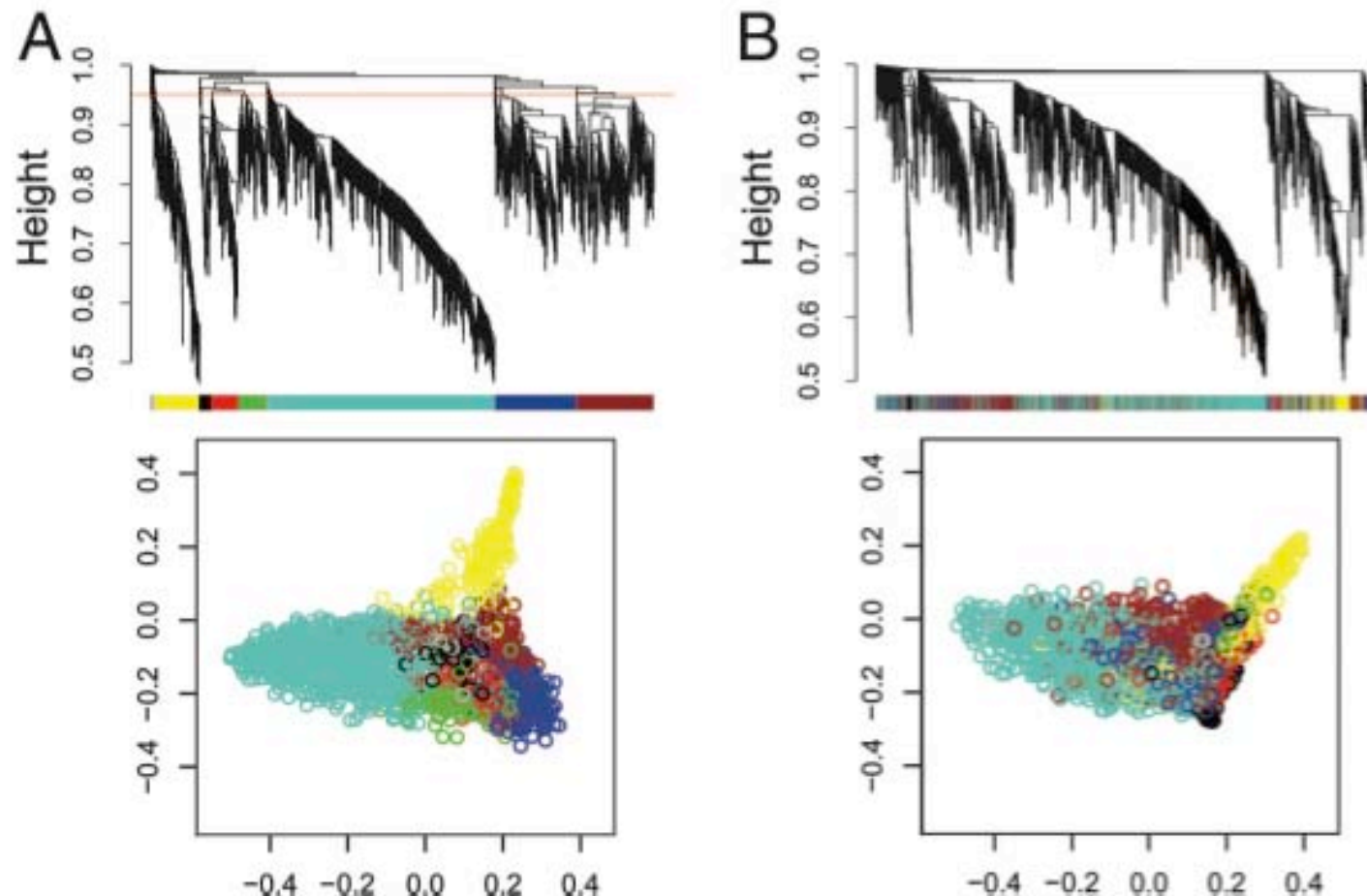
Conservation and evolution of gene coexpression networks in human and chimpanzee brains

Oldham M, Horvath S, Geschwind DH

Proc Natl Acad Sci USA

2006 vol. 103 (47) pp. 17973-8

Fig. 1. Network analysis of gene expression in human and chimpanzee brains identifies distinct modules of coexpressed genes in human (A) and chimpanzee (B). (A) Dendrograms produced by average linkage hierarchical clustering of 2,241 genes based on TO (see *Supporting Text*). The red line in the human dendrogram indicates the height at which the tree was cut (0.95) to define modules. Modules were assigned colors as indicated in the horizontal bar beneath the human dendrogram. Genes in the chimpanzee network are depicted by using human module colors to represent the extent of module conservation. (B) Classical multidimensional scaling plots in three dimensions (color-coded as in A) depict the relative size and cohesion of modules in humans and chimpanzees.



Conservation and evolution of gene coexpression networks in human and chimpanzee brains

Oldham M, Horvath S, Geschwind DH

Proc Natl Acad Sci USA

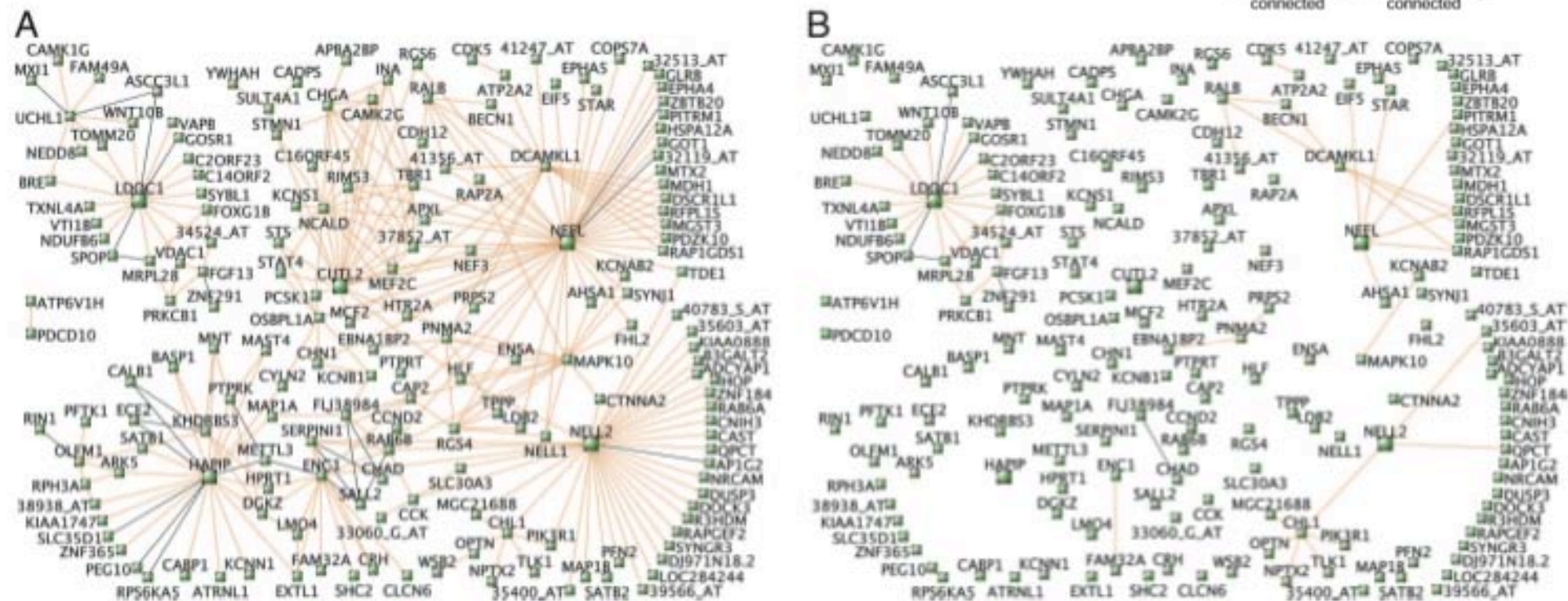


Fig. 3. Module visualization identifies hub genes and human-specific connections. (A) Three hundred pairs of genes with the greatest TO in humans are depicted for cortex (brown module). Genes with expression levels that are negatively correlated are connected by black lines. Where gene symbols are unknown, Affymetrix probe set IDs are shown (e.g., 37158_at). (B) Connections from A that are present in humans but absent in chimpanzees (see Materials and Methods).

NRG1: Glycoprotéine de 44kD, signalisation, développement, impliquées dans plusieurs maladies dont cancer, **schizophrénie and psychose maniaco-dépressive**

LDOC1 : Protéine nucléaire, **développement, cancer**

EYA1 : Facteur de transcription **développement, vision (œil)**

LECT1 : Glycoprotéine, angiogenèse, **vascularisation** au cours du développement

PGAM2 : Phosphoglycerate mutase (PGAM), stockage du **glycogène**

COX5A : Protéine **mitochondriale**, ETC

COX6A2 : Protéine **mitochondriale**, ETC

UQCRCFS1 : Protéine **mitochondriale, cancer , schizophrénie**

IMMT : Protéine **mitochondries**, morphologie des mitochondries, interagit avec DISC1
(Disrupted in **Schizophrenia** 1)

DNM1L : Membre de la superfamille des dynamin sf GTPases, morphologie **mitochondriale**

DTNA1 : Dystrobrevin A1, muscle, **CNS, développement** de l'œil, de l'oreille interne, de l'hypophyse, de la barrière hémato méningée, plus d'autres régions cérébrales.

RAB3A : Exocytose, fusion des **vésicules**

ABI2 : **Cytosquelette actine**

CYFIP2 : **Cytosquelette**, interagit avec FRMP, **retard mental**

MAP1B : Polymérisation des **microtubules**

FGF12 : Membre de la famille des FGF avec localisation nucléaire

SLC30A9 : Transporteur, Zinc

ANKMY2 : Ankyrin repeat, pourrait être impliquée dans le transport de protéines de **signalisation** par les cils

KIAA1279 : Famille des kinésines (moteur moléculaire), transport des **mitochondries**, mutations associées au **Goldberg-Shprintzen megacolon syndrome** (maladie rare, affectant aussi le SNC)

**Human brain evolution:
harnessing the genomics
(r)evolution to link genes,
cognition, and behavior**

Neuron
2010 vol. 68 (2) pp. 231–44

Konopka G, Geschwind DH

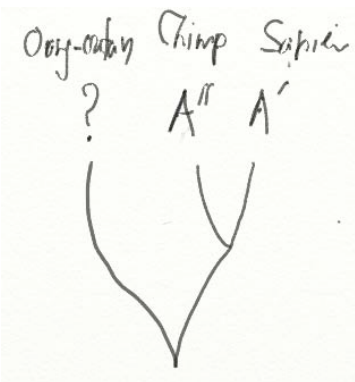
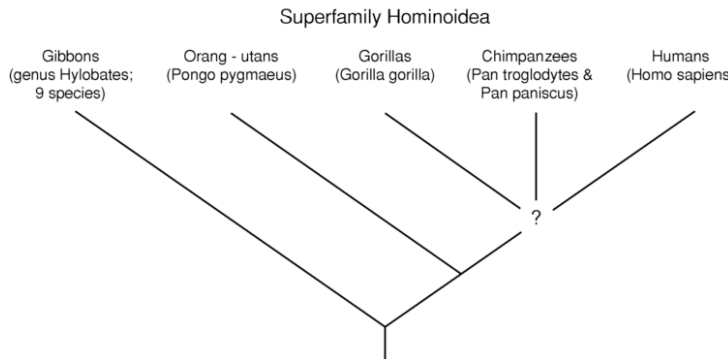
Studying the brain from an evolutionary perspective and combining these results with those from development and pathology, connecting genetic variation to neural circuit development and functioning, will yield the best approximation of how natural forces shaped this organ. Aside from satisfying basic curiosity about the origins of our abilities, such endeavors have enormous implications for understanding human diseases involving cognition and behavior, ranging from intellectual disability and autism to neurodegenerative dementias.

Human brain evolution: harnessing the genomics (r)evolution to link genes, cognition, and behavior

Konopka G, Geschwind DH

Neuron

2010 vol. 68 (2) pp. 231-44



| Common Name | Species | Original Date Sequenced | Unique Features |
|----------------|--------------------------------|-------------------------|--|
| Mouse | <i>Mus musculus</i> | 2002 | Common model system for neurobehavioral/ neurogenetic experiments |
| Human | <i>Homo sapiens</i> | 2001 | |
| Rat | <i>Rattus norvegicus</i> | 2003 | Common model system for neurobehavioral experiments; now available for genetic manipulations |
| Fly | <i>Drosophila melanogaster</i> | 2003 | Common model system for neurobehavioral/ neurogenetic experiments |
| Worm | <i>Caenorhabditis elegans</i> | 2004 | Aging and longevity |
| Chimpanzee | <i>Pan troglodytes</i> | 2005 | Great ape; most similar to human on genome level |
| Zebrafish | <i>Danio rerio</i> | 2005 | Easy to visualize brain development; behavior; genetically malleable |
| Rhesus macaque | <i>Macaca mulatta</i> | 2006 | Old world monkey; bred in the USA for behavior and neurophysiology experiments |
| Honey bee | <i>Apis mellifera</i> | 2006 | Social behavior; aggression |
| Orangutan | <i>Pongo pygmaeus abelii</i> | 2007 | Great ape; useful for outgroup comparison with human/chimp |
| Elephant shark | <i>Callorhinichthys milii</i> | 2007 | Outgroup for zebrafish and mouse comparisons |
| Dolphin | <i>Tursiops truncatus</i> | 2008 | Evidence for vocalization and self-awareness |
| Zebra finch | <i>Taeniopygia guttata</i> | 2008 | Patterned vocalization |
| Sea hare | <i>Aplysia californica</i> | 2008 | Learning and memory |
| Elephant | <i>Loxodonta africana</i> | 2009 | Evidence for vocalization and self-awareness |
| Pig | <i>Sus scrofa</i> | 2009 | Gyrencephalic cortex |
| Bat | <i>Myotis lucifugus</i> | 2010 | Echolocation |
| Ferret | <i>Mustela putorius furo</i> | in progress | Gyrencephalic cortex |
| Cichlids | <i>Tilapia nilotica</i> | in progress | "Natural" mutants for the study of evolution |
| Marmoset | <i>Callithrix jacchus</i> | in progress | New world monkey |

Human brain evolution: harnessing the genomics (r)evolution to link genes, cognition, and behavior

Konopka G, Geschwind DH

Neuron

2010 vol. 68 (2) pp. 231–44

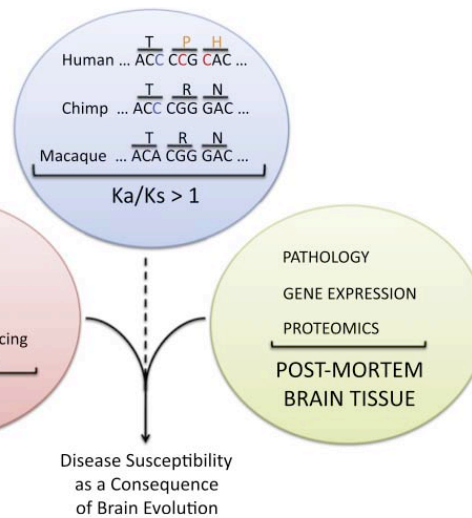


Figure 1. Combining Comparative Genomics with Phenotype and Expression Data Leads to Disease Insights

Measures of positive selection are typically calculated by dividing the number of nonsynonymous changes (depicted in red) by the number of synonymous changes (depicted in blue); a value greater than one is used as evidence for positive selection. It should be emphasized that this is arbitrary and only takes into account known protein coding regions. Screening genomes for genes under positive selection is one important step; however, other measures such as links to behavior and expression need to be incorporated. Furthermore, a gene does not have to have undergone positive selection to be a disease-susceptibility gene. Other changes in evolution such as timing or location of expression could make a gene or signaling pathway vulnerable in disease.

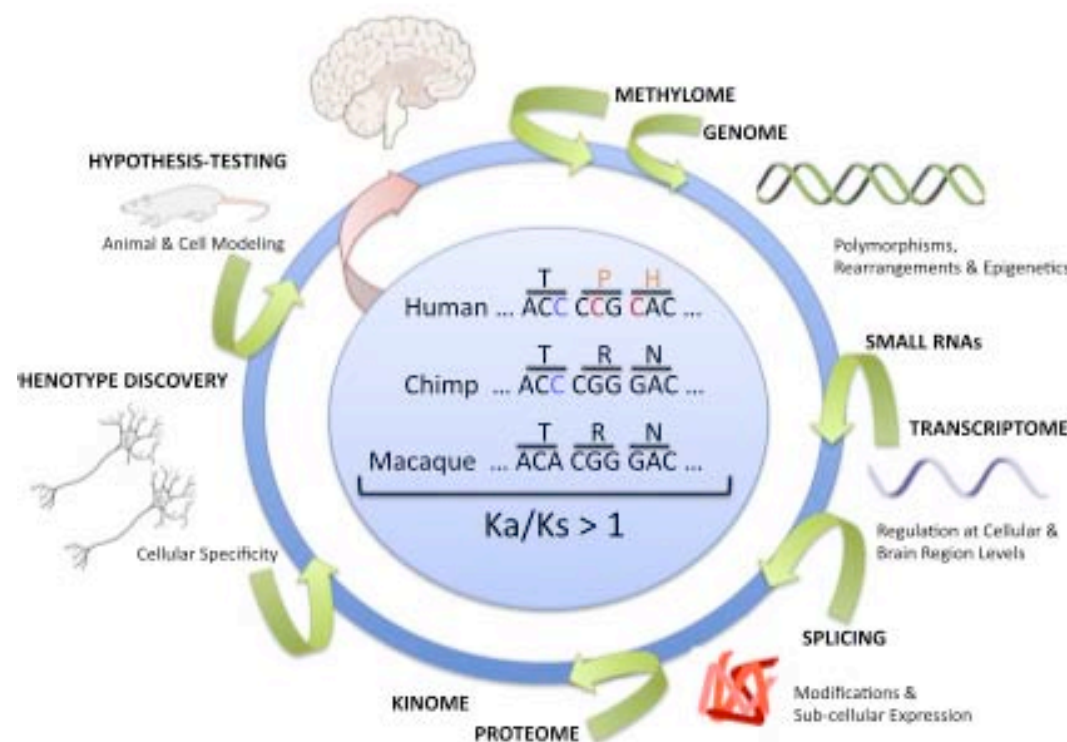


Figure 2. Multiple Layers of Regulation Underlie Human Brain Evolution

More than genomic comparisons need to be considered when building our understanding of human brain evolution. Regulation at the level of the epigenome (e.g., methylome), regulation of expression by changes in transcription or small RNA regulation, novel isoforms through differential splicing, changes in regional and subcellular expression, and posttranslational modifications (e.g., kinome) all need to be taken into account, and many of these changes can be queried using NGS techniques. Also, the incorporation of animal models and cell-specific lines of inquiry need to be undertaken. Finally, the integration of all of these data will lead to phenotype discovery and hypothesis-testing that ultimately will inform polymorphism discovery in human brain diseases. In this manner, modern neurogenetic investigations are not only an exercise in advanced data analysis, but comprehensive data integration.

Both noncoding and protein-coding RNAs contribute to gene expression evolution in the primate brain

Babbitt CC, Fedrigo O, Pfeiferle AD, Boyle AP,
Horvath JE, Furey TS, Wray G

Categorical Enrichment To determine functional category enrichment for the differentially expressed genes, we employed the PANTHER (HMM Library Version 6.0; Mi et al. 2005) and GO (The Gene Ontology Consortium, 2000) gene ontology databases. Our background set of genes were those genes measured in our tissue samples. PANTHER and GO category enrichment scores were computed using the top 5% of the hypergeometric probability distribution. Python code used to perform all enrichments is available at: http://www.duke.edu/~ofedrigo/Olivier_Fedrigo/PythonScripts.html.

Note.—The results for the biological process domain of both the GO and PANTHER ontologies are shown. Categorical enrichments are for the top 5% of a hypergeometric probability distribution. The right-hand columns show the number of genes in the top 5%, as well as the total number of genes evaluated. Categories that evaluated less than 10 genes total are not shown. Categories are further colored according to hierarchically related ontology terms: nucleic acid metabolism (green), electron transport (yellow), neuronal activity (blue), transport, extra- and intracellular protein traffic (pink), and lipid metabolism (purple).

Genome Biol Evol
2010 vol. 2 pp. 67–79

Categorical Enrichments for Differentially Expressed Genes between the Human and Chimpanzee Individuals

| Category | P value | Top 5.0% | Total |
|---|--------------------------|----------|-------|
| PANTHER | | | |
| DNA repair | 8.06 × 10 ⁻⁰⁵ | 17 | 119 |
| DNA metabolism | 9.58 × 10 ⁻⁰⁵ | 26 | 233 |
| Intracellular protein traffic | 0.0001132 | 61 | 759 |
| Electron transport | 0.007361 | 16 | 163 |
| Neurotransmitter release | 0.01398 | 10 | 90 |
| Oxidative phosphorylation | 0.01562 | 7 | 53 |
| Induction of apoptosis | 0.01983 | 10 | 95 |
| Endocytosis | 0.02428 | 17 | 202 |
| Extracellular transport and import | 0.03121 | 6 | 48 |
| Protein targeting and localization | 0.03184 | 14 | 162 |
| Nuclear transport | 0.03957 | 7 | 64 |
| Cytokinesis | 0.04562 | 7 | 66 |
| GO | | | |
| Translational elongation | 0.0004988 | 11 | 68 |
| Viral genome replication | 0.002211 | 4 | 12 |
| Protein import into nucleus, docking | 0.008714 | 4 | 17 |
| Phospholipid metabolic process | 0.01311 | 4 | 19 |
| Transport | 0.0139 | 34 | 460 |
| Glutamate signaling pathway | 0.01946 | 3 | 12 |
| Induction of apoptosis | 0.02269 | 10 | 97 |
| Intracellular protein transport | 0.02412 | 14 | 156 |
| tRNA aminoacylation for protein translation | 0.02438 | 3 | 13 |
| Lipid catabolic process | 0.02472 | 7 | 58 |
| Nucleocytoplasmic transport | 0.0299 | 3 | 14 |
| Regulation of GTPase activity | 0.03603 | 3 | 15 |
| Electron transport chain | 0.04029 | 8 | 78 |
| RNA processing | 0.04054 | 6 | 51 |
| Base-excision repair | 0.04274 | 3 | 16 |
| Inactivation of MAPK activity | 0.04274 | 3 | 16 |
| Protein stabilization | 0.04274 | 3 | 16 |
| DNA repair | 0.04792 | 11 | 125 |
| Phospholipid biosynthetic process | 0.04874 | 4 | 28 |

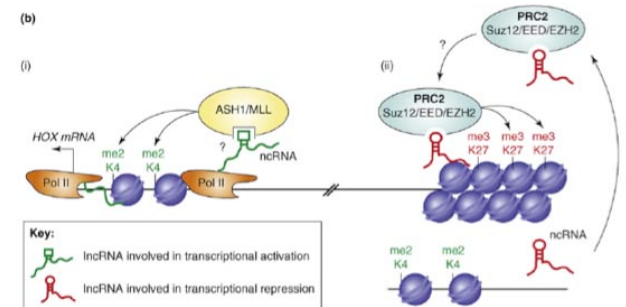
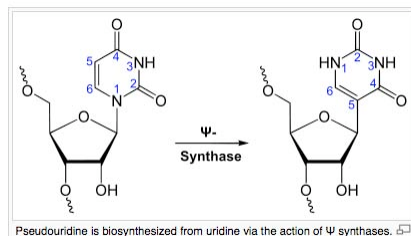
Table 1 | Types of ncRNAs*

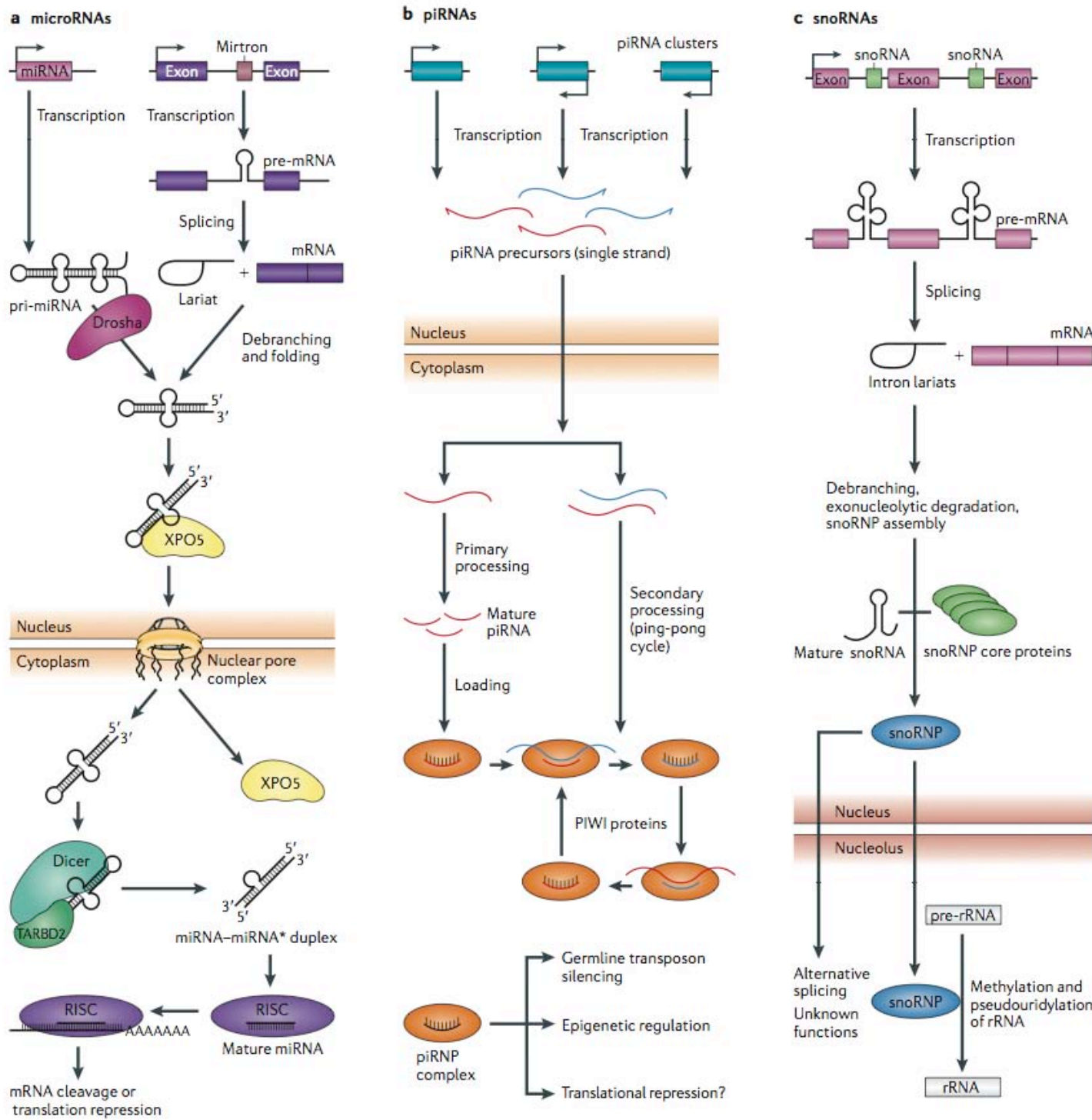
| Name | Size | Location | Number in humans | Functions | Illustrative examples | Refs |
|------------------------|-----------|------------------------------------|------------------|---|--|---------|
| Short ncRNAs | | | | | | |
| miRNAs | 19–24 bp | Encoded at widespread locations | >1,424 | Targeting of mRNAs and many others | miR-15/16, miR-124a, miR-34b/c, miR-200 | 3–8 |
| piRNAs | 26–31 bp | Clusters, intragenic | 23,439 | Transposon repression, DNA methylation | piRNAs targeting <i>RASGRF1</i> and LINE1 and IAP elements | 13–19 |
| tiRNAs | 17–18 bp | Downstream of TSSs | >5,000 | Regulation of transcription? | Associated with the CAP1 gene | 37 |
| Mid-size ncRNAs | | | | | | |
| snoRNAs | 60–300 bp | Intronic | >300 | rRNA modifications | U50, SNORD | 20–22 |
| PASRs | 22–200 bp | 5' regions of protein-coding genes | >10,000 | Unknown | Half of protein-coding genes | 10 |
| TSSa-RNAs | 20–90 bp | −250 and +50 bp of TSSs | >10,000 | Maintenance of transcription? | Associated with <i>RNF12</i> and <i>CCDC52</i> genes | 35 |
| PROMPTs | <200 bp | −205 bp and −5 kb of TSSs | Unknown | Activation of transcription? | Associated with <i>EXT1</i> and <i>RBM39</i> genes | 36 |
| Long ncRNAs | | | | | | |
| lncRNAs | >200 bp | Widespread loci | >1,000 | Examples include scaffold DNA–chromatin complexes | <i>HOTAIR</i> , <i>HOTTIP</i> , lncRNA-p21 | 2,28–30 |
| T-UCRs | >200 bp | Widespread loci | >350 | Regulation of miRNA and mRNA levels? | uc.283+, uc.338, uc160+ | 31–34 |
| Other lncRNAs | >200 bp | Widespread loci | >3,000 | Examples include X-chromosome inactivation, telomere regulation, imprinting | <i>XIST</i> , <i>TSIX</i> , TERRAs, p15AS, <i>H19</i> , <i>HYMAI</i> | 2,23–25 |

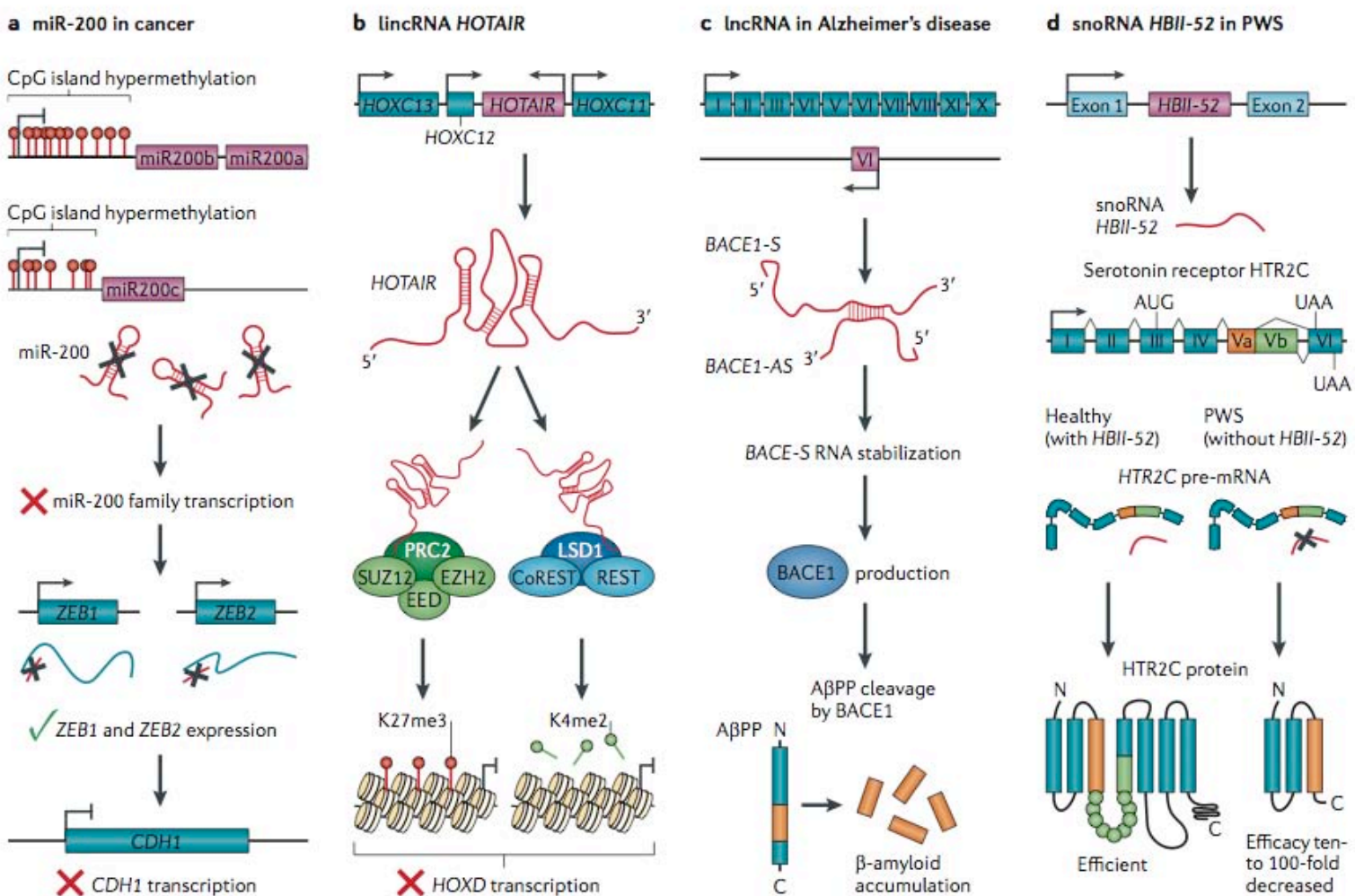
Non-coding RNAs in human disease

Esteller M

Nature Reviews Genetics 12, 861 (2011). doi: 10.1038/nrg3074





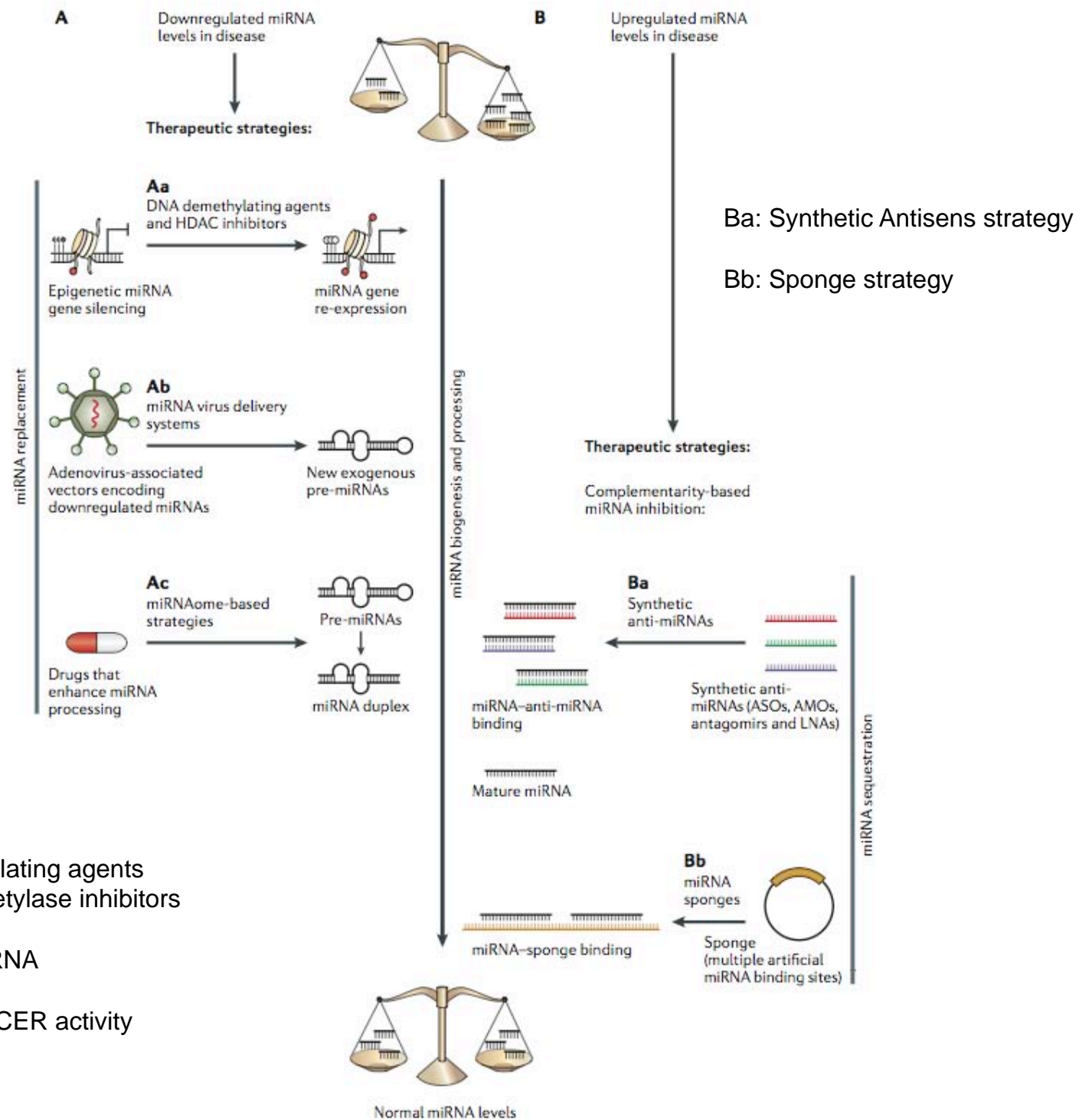


invasiveness. **c |** lncRNA targeting of β -secretase 1 (BACE1) has a role in the pathophysiology of Alzheimer's disease. An antisense lncRNA, BACE1-AS, regulates the expression of the sense BACE1 gene (labelled BACE1-S in the figure) through the stabilization of its mRNA. BACE1-AS is elevated in Alzheimer's disease, increasing the amount of BACE1 protein and, subsequently, the production of β -amyloid peptide. **d |** The role of the snoRNA in Prader-Willi syndrome (PWS). The loss of the snoRNA in PWS changes the alternative splicing of the serotonin receptor HTR2C precursor mRNA (pre-mRNA), resulting in a protein with reduced function. A β PP, amyloid- β precursor protein; CoREST, REST corepressor.

Table 3 | Illustrative list of ncRNAs that are disrupted in non-tumoural disorders

| Disease | Involved ncRNAs | ncRNA type | Refs |
|---------------------------------------|--|------------|---------|
| Spinal motor neuron disease | miR-9 | miRNA | 87 |
| Spinocerebellar ataxia type 1 | miR-19, miR-101, miR-100 | miRNA | 88 |
| Amyotrophic lateral sclerosis | miR-206 | miRNA | 86 |
| Arrhythmia and hypertension | miR-1 | miRNA | 98 |
| Atheromatosis and atherosclerosis | miR-10a, miR-145, miR-143 and miR-126 | miRNA | 100–102 |
| Atheromatosis and atherosclerosis | Circular ncRNA linked to the CDKN2A locus | lncRNA | 119 |
| Cardiac hypertrophy | miR-21 | miRNA | 144 |
| Rett's syndrome | miR-146a, miR-146b, miR-29 and miR-382 | miRNA | 108,109 |
| 5q syndrome | miR-145 and miR-146a | miRNA | 106 |
| ICF syndrome | miR-34b, miR-34c, miR-99b, let-7e and miR-125a | miRNA | 107 |
| Crohn's disease | miR-196 | miRNA | 110 |
| Prader–Willi and Angelman syndromes | snoRNA cluster at 15q11–q13 imprinted locus | snoRNA | 114–116 |
| Beckwith–Wiedeman syndrome | lncRNAs H19 and KCNQ1OT1 | lncRNA | 145 |
| Uniparental disomy 14 | snoRNA cluster at 14q32.2 imprinted locus | snoRNA | 145 |
| Silver–Russell syndrome | lncRNA H19 | lncRNA | 145 |
| Silver–Russell syndrome | miR-675 | miRNA | 145 |
| McCune–Albright syndrome | lncRNA NESP-AS | lncRNA | 145 |
| Deafness | miR-96 | miRNA | 111 |
| Alzheimer's disease | miR-29, miR-146 and miR-107 | miRNA | 89–91 |
| Alzheimer's disease | ncRNA antisense transcript for BACE1 | lncRNA | 112 |
| Parkinson's disease | miR-7, miR-184 and let-7 | miRNA | 82 |
| Down's syndrome | mir-155 and miR-802 | miRNA | 83 |
| Idiopathic neurodevelopmental disease | T-UCRs uc.195, uc.392, uc.46 and uc.222 | T-UCR | 113 |
| Rheumatoid arthritis | miR-146a | miRNA | 147 |
| Transient neonatal diabetes mellitus | lncRNA HYMAI | lncRNA | 148 |
| Pseudohypoparathyroidism | lncRNA NESP-AS | lncRNA | 146 |

BACE1, β -secretase 1; CDKN2A, cyclin-dependent kinase inhibitor 2A; HYMAI, hydatidiform mole associated and imprinted; ICF syndrome, immunodeficiency, centromeric region instability and facial anomalies syndrome; KCNQ1OT1, KCNQ1 opposite strand/antisense transcript 1; lncRNA, long non-coding; miRNA, microRNA; NESP, also known as GNAS; NESP-AS, NESP antisense; ncRNA, non-coding RNA; snoRNA, small nucleolar RNA; T-UCR, transcribed ultraconserved region.





Source: Suzanne Stensaas et O.E. Millhouse, The Digital Slice of Life

